ACS OMEGA

http://pubs.acs.org/journal/acsodf

Article

Aberrant Fucosylation of Saliva Glycoprotein Defining Lung Adenocarcinomas Malignancy

Ziyuan Gao, Zhen Wu, Ying Han, Xumin Zhang, Piliang Hao, Mingming Xu, Shan Huang, Shuwei Li, Jun Xia, Junhong Jiang,* and Shuang Yang*

Cite This: *ACS Omega* 2022, 7, 17894−17906

Read Online

ACCESS | Metrics & More | Article Recommendations | Supporting Information

ABSTRACT: Aberrant glycosylation is a hallmark of cancer found during tumorigenesis and tumor progression. Lung cancer (LC) induced by oncogene mutations has been detected in the patient's saliva, and saliva glycosylation has been altered. Saliva contains highly glycosylated glycoproteins, the characteristics of which may be related to various diseases. Therefore, elucidating cancer-specific glycosylation in the saliva of healthy, non-cancer, and cancer patients can reveal whether tumor glycosylation has unique characteristics for early diagnosis. In this work, we used a solid-phase chemoenzymatic method to study the glycosylation of saliva glycoproteins in clinical specimens. The results showed that the α1,6-core fucosylation of glycoproteins was increased in cancer patients, whereas α1,2 or α1,3 fucosylation was significantly increased. We further analyzed the expression of fucosyltransferases responsible for α1,2, α1,3, and α1,6 fucosylation. The fucosylation of the saliva of cancer patients is drastically different from that of non-cancer or health controls. These results indicate that the glycoform of saliva fucosylation distinguishes LC from other diseases, and this feature has the potential to diagnose lung adenocarcinoma.

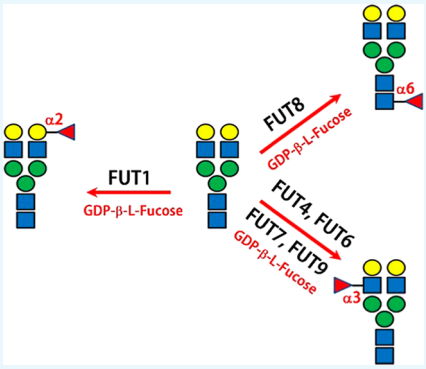

INTRODUCTION

As one of the common post-translationally modifications, glycosylation is associated with many diseases, and its abnormal changes can affect the pathophysiology of cells or organisms.[1,2] Changes in glycosylation play a vital role in diseases such as increased fucosylation in prostate cancers,[3,4] dysregulated glycoforms in influenza virus,[5,6] varied glycosites of spike glycoprotein in COVID-19,[7,8] upregulated sialylation in cardiovascular disease,[9] and elevated *O*-GlcNAcylation in neurodegenerative disease.[10,11] In particular, protein glycosylation changes during tumorigenesis and cancer progression.[12,13] Therefore, disease-specific glycosylation is often used as a diagnostic and/or prognostic biomarker. For instance, the core fucosylation of α-fetoprotein (AFP) is a clinical molecule for liver cancer diagnosis; using AFP core fucosylation instead of total AFP can improve sensitivity and specificity.[14] Since most tumor markers approved by Food and Drug Administration are glycoproteins, such as cancer antigen 125 (CA 125), AFP, immunoglobulins, neuron-specific enolase, and prostate-specific antigen (PSA), potential cancer biomarkers are likely to be glycoproteins in human biofluids.[15−17] Glycoenzymes [glycosyltransferases (GTFs) and glycosidases] may be intrinsically regulated in the tumor microenvironments.[18,19] Dysregulated glycoenzymes and their protein expression can alter protein glycosylation, leading to changes in the function of the protein cascade in the cell. Thus, analysis of tumor-specific glycosylation and upstream glycoenzymes is important to identify potential biomarkers for diagnosis and prognosis.

For non-invasive detection of body fluids, liquid biopsy has become a very popular focus in recent years, such as blood, circulating tumor cells, and circulating tumor DNA (ct DNA). Studies have shown that the early diagnosis of different cancers can be achieved by detecting ctDNA methylation in longitudinal studies in patient plasma.[20] Tumor markers can also be proteins or other substances that are present or produced in cancer or other cells of the body in response to the tumor microenvironment. Glycosylation is also used as a detection in various cancer liquid biopsies as tumor-associated glycans or glycoproteins may be secreted into the circulation and present in different body fluids as potential biomarkers. Therefore, human plasma, urine, and saliva can all be used to discover disease-specific glycosylation markers. Plasma markers such as PSA, CA-125, AFP, or amyloid-beta precursor protein have been clinically used for the early detection of prostate cancer, ovarian cancer, liver cancers, and Alzheimer's disease, respectively.[21,22] Recent studies have found that the expression

Received: February 28, 2022
Accepted: May 11, 2022
Published: May 19, 2022

of serum proteins CEA (carcinoembryonic antigen), RBP (retinol-binding protein), and α1 antitrypsin in the diagnosis of lung cancer (LC) has a sensitivity of 89.3% and a specificity of 84.7%.[23] The results are based on the analysis of the serum proteins of several patients diagnosed with non-small-cell LC (NSCLC). However, more clinical studies are needed to confirm whether these results are applicable to different subtypes of NSCLC.

In addition to serum or plasma, which is widely used for biomarker discovery, saliva has become one of the essential biofluids in diagnosis due to non-invasive sample preparation. It can avoid the pain, anxiety, or risk of infection, and it is easy to store and collect multiple subsequent specimens. Saliva has been used to diagnose oral diseases and monitor disease progression, such as periodontal pathogen[24] or patients suspected COVID-19.[25,26] Proteomic analysis of human saliva found that 48 out of the 500 proteins were differentially expressed between healthy controls (HCs) and gastric cancer patients. Among them, STAT2 (signal transducer and activator of transcription 2) was upregulated, and the tumor suppressor of DMBT1 (deleted in malignant brain tumors 1 protein) was downregulated.[27] STAT family members such as STAT2 play an important role in the regulation of cell proliferation, differentiation, apoptosis, and angiogenesis.[28] For example, upregulation of TLR2 driven by STAT3 can promote gastric tumorigenesis, and inhibition of STAT3 signaling can prevent gastric cancer proliferation and metastasis.[29,30] A meta-analysis of 29 articles from more than 10,000 subjects showed that the diagnostic accuracy of saliva biomarkers for LC remote from the mouth is up to 88%.[31] Therefore, saliva is a promising non-invasive biofluid for discovering novel biomarkers for LC.

In addition to urea, ammonia, and electrolytes, saliva also contains many proteins. The most abundant saliva proteins are mucins, amylases, defensins, cystatins, histatins, proline-rich proteins, statherin, lactoperoxidase, lysozyme, lactoferrin, and immunoglobulins. These proteins can come from the salivary gland, stomach, and lung.[32,33] Mass spectrometry (MS) analysis of exosomes and macrovesicles in the saliva of LC patients revealed that approximately 4% of the identified proteins belonged to distal lung cells. Among them, BPIFA1 (BPI fold-containing family A member 1), CRNN (cornulin), MUC5B (mucin-5B), and IQGAP (Ras GTPase-activating-like protein) are dysregulated in LC, and most of which are also glycosylated.[34] The changes in glycosylation may be attributed to the differential expression of glycoenzymes and their substrates in the tumor environment. GTFs, such as glucosyltransferase B (GtfB),[35] α1,3-fucosyltransferase (FUT5),[36] α1,3-mannosyltransferase (ALG3), *N*-acetylgalactosaminide α2,6-sialyltransferase 1 (ST6GALNAC1), and α-*N*-acetyl-neuraminide α2,8-sialyltranserase 2 or 5 (ST8SIA2 or ST8SIA5) (the Human Protein Atlas), are highly abundant in saliva. Glycosylation of saliva-containing microbe, phagocyte, mucin, or agglutinin is regulated by these GTFs.[37] Saliva glycoproteins, MUC5B, MUC7 (mucin-7),[38] salivary agglutinin (SAG),[39] β-2-micoglobulin,[40] and proline-rich glycoprotein,[38] can change when tumor initializes and progresses further through dysregulated glycoenzymes. Consequently, the identification of tumor-specific glycosylation and its dependent regulators is crucial for the discovery of biomarkers of interest.

We hypothesized that tumor-associated glycosylation exists in saliva that can be used to differentiate lung adenocarcinoma patients from healthy individuals. To decipher protein glycosylation, structural analysis of glycans, glycosites, site occupancy, and occupied glycans of glycosites is required. Glycan analysis can be performed by glycosidases or alkaline β-elimination,[41,42] while *N*-glycosites are determined by tandem MS (MS/MS) against the intact *N*-glycopeptides enriched by hydrophilic interaction liquid chromatography.[43−45] Complex O-glycosylation has been successfully studied by O-protease (OpeRATOR or StcE), which cleaves the N-terminus of *O*-glycosylated serine or threonine; *O*-glycopeptides are usually analyzed by electron-transfer and higher-energy collision dissociation (EThcD) fragmentation.[46−48] Conversely, the linkages of labile sialic acids are differentially derivatized by ethyl esterification and reductive amination using amine-containing compounds.[49,50] The derivatization of sialic acid on the solid phase not only stabilizes the α-2,3 and α-2,6 linkages sequentially but also facilitates the removal of reagents after the reaction.[50] By combining these analytical platforms and advanced MS technology, we can extensively deconvolute disease-specific glycopatterns by comparing protein glycosylation between HCs and non-cancer and cancer patients.

In this study, we used a solid-phase chemoenzymatic method to compare saliva glycosylation in HCs and non-cancer and cancer patients. To determine the linkage of fucosylation, glycoproteins are conjugated to a solid support, and their fucoses are sequentially digested by specific α-fucosidases. Unstable sialic acids are modified by two-step chemical derivatization, and the linkages between α2,6 and α2,3 are distinguished by carrying a distinct mass tag after derivatization. Fucosylated glycoproteins are studied by bottom-up proteomics and matrix-assisted laser desorption/ionization (MALDI)-MS. Fucosyltransferases are quantitatively analyzed by qPCR. The biosynthesis of fucosylated high-mannose or complex *N*-glycans and their potential application for diagnosis of LC are also discussed.

METHODS

Participants and Study Design. The workflow of clinical samples is shown in Figure 1. In this study, saliva samples were collected from 51 individuals, including 20 patients with LC, 21 patients with other diseases, and 10 healthy volunteers. Saliva samples were divided into HC, other non-cancer disease (OD), and lung adenocarcinomas (LC) (see Supporting Information Table S1). All patients in the LC group were histopathologically confirmed as lung adenocarcinoma, has no history of inflammatory disease or other malignant tumors, and had not received chemotherapy or radiotherapy. In this study, there was statistically no significant difference between LC and OD/HC in terms of gender, smoking history, and other factors. All patient samples were collected according to protocols approved by the Institutional Review Board (IRB) of the First Affiliated Hospital of Soochow University, and written informed consent was provided to patients in advance.

Standard Procedure for Saliva Collection. All saliva samples were collected in the morning (9−11 am). Patients and healthy individuals were asked not to eat, drink, smoke, or use any oral cleaning products for at least 1 h before collecting saliva. This minimizes the effect of smoking, food, alcohol consumption, or beverages on the final results of the experiment. Subjects rinsed their mouth 2−3 times with drinking water 5 min before collection to ensure oral hygiene. In the absence of stimulation, naturally secreted whole saliva was collected in a 50 mL centrifuge tube. Saliva collection (∼5 mL) must be completed within 10 min. During the collection process, the saliva collected in the centrifuge tube must be kept

https://doi.org/10.1021/acsomega.2c01193
ACS Omega 2022, 7, 17894−17906

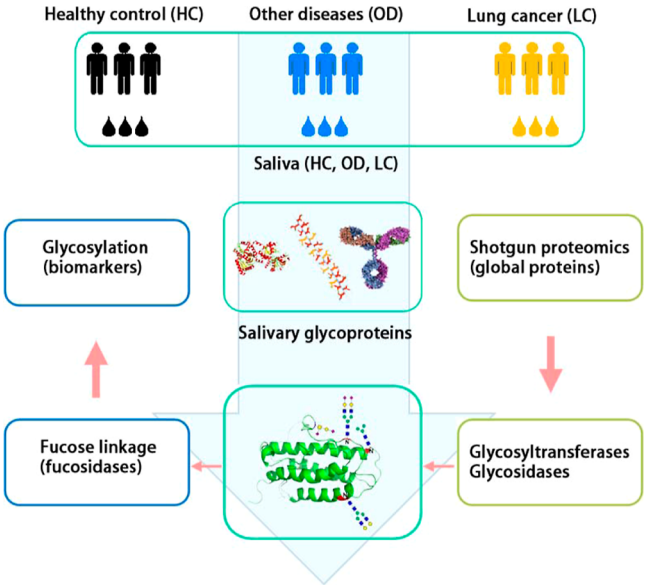

Figure 1. MS workflow for analysis of saliva proteins, glycoproteins, and glycans. Three groups have been used for comparison, including HC, OD, and LC. First, proteins are extracted from saliva and used for glycosylation analysis, bottom-up (or shotgun) proteomics, and fucosylation linkage determination. Shotgun proteomics can identify GTFs responsible for specific glycosylation.

on ice. Saliva samples were centrifuged at 12,000 rpm for 25 min at 4 °C. After discarding the pellet and adding 100× protease inhibitor to the supernatant, the saliva samples are stored at −80 °C.

SDS-PAGE and Glycosidase Treatment of Saliva Proteins. The concentration of saliva proteins was measured by bicinchoninic acid (BCA) assay and nanodrop. Three sets of saliva samples were diluted to a concentration of ∼1 mg/μL. 20 μg of protein was taken from each group and reacted with PNGase F, fucosidase, and a mixture of the two enzymes at 37 °C for 4 h. The 5× protein loading buffer was added to the saliva with and without these enzyme digestion, and samples were incubated at 100 °C for 5 min. Electrophoresis was performed on SDS-PAGE using 10% SDS-PAGE gel kit (Beyotime). Running buffer consists of 0.025 M Tris, 0.192 M glycine, and 0.1% SDS. 20 μL mixture of the sample (20 μg) and loading buffer was added to the gel well. After electrophoresis, the gel was stained in the staining solution (containing 0.25% Coomassie Bright Blue R250, 45% methanol, and 10% acetic acid) for 3 h and then eluted in the eluting buffer (methanol/glacial acetic acid/water = 2:2:9, v/v) until protein bands were clear. The gel bands were then imaged using the ChemiDoc MIP imaging system (Bio-Rad).

Saliva Protein Extraction. The 500 μL of solution consists of trichloroacetic acid (20% w/v), acetone (90% v/v), and dithiothreitol (DTT; 20 mM) and was mixed with 500 μL saliva. The mixture was vortexed and precipitated overnight at −20 °C. The sample was then centrifugated at 15,000 rpm for 30 min at 4 °C. The supernatant was discarded, and the pellet was collected, then washed with 200 μL of cold acetone (90%) and 20 mM DTT, and finally washed with cold acetone (80%) and 10 mM DTT. To suspend the pellet in the solution, the sample was sonicated for at least 5 min prior to acetone-DTT wash. The pellet was placed at −20 °C for 20 min, then centrifugated at 15,000 rpm for 5 min at 4 °C. Finally, the

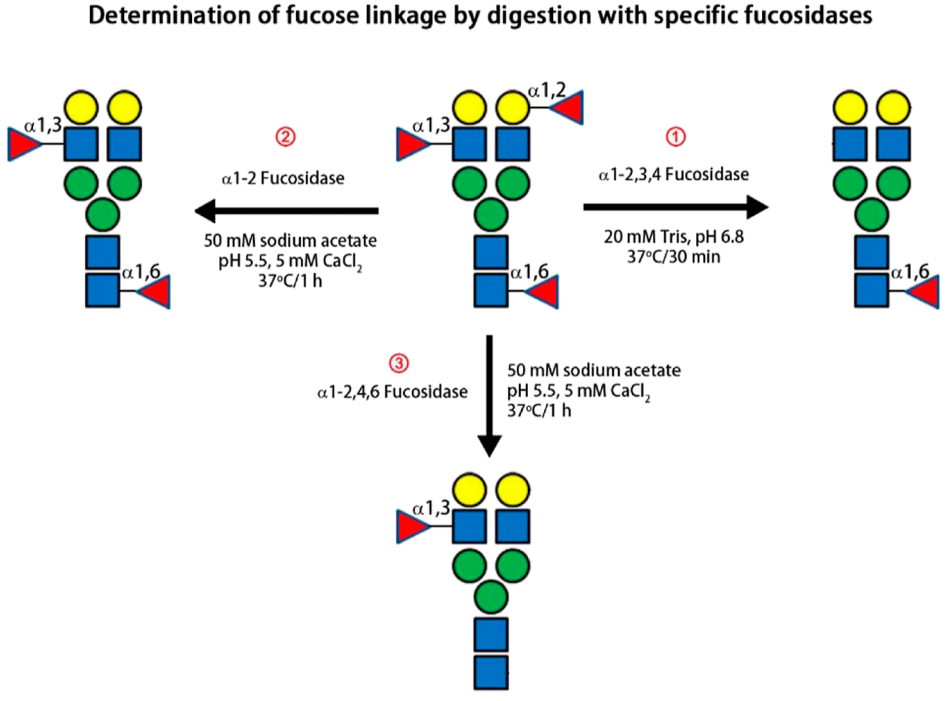

Figure 2. Schematic diagram of determination of fucosylation linkage using specific fucosidase and MS analysis. ① Removal of all fucose linkages except for core α1,6 fucosylation by α1-2,3,4 fucosidase. This scheme led to the determination of core α1,6 linkage of fucosylated glycan; ② removal of α1,2 linkage of fucosylated glycan by α1-2 fucosidase. The remaining linkages of fucosylation can be α1,3 or α1,6. The α1,3 is then determined by comparing fucosylated glycans with scheme 1; and ③ removal of all linkages except for α1,3Fuc-GlcNAc through α1-2,4,6 fucosidase. This scheme confirms whether there is α1,4 linkage.

https://doi.org/10.1021/acsomega.2c01193
ACS Omega 2022, 7, 17894−17906

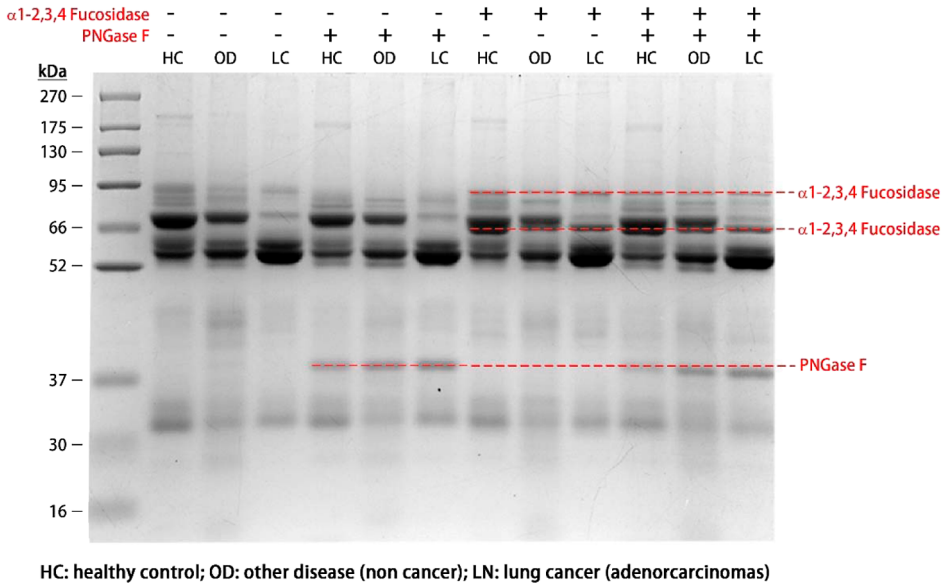

Figure 3. Different glycosylation present in saliva glycoproteins in HC, non-cancer, and LC. Proteins of HC, OD, and LC were treated with PNGase F, α1-2,3,4 fucosidase. PNGase F removes *N*-glycans from glycoproteins, thereby reducing the MW of *N*-glycoproteins. α1-2,3,4 Fucosidase hydrolyzes fucose with linkages of α1-2, α1-3, or α1-4. A decrease in the MW of glycoproteins suggests one or more of these fucosylated linkages but not α1-6. The MW of PNGase F is about 36 kDa, while α1-2,3,4 Fucosidase consists of two fucosidases modified with His-tags, with the MW of 87 and 64 kDa.

pellet was collected and dried in a Speed-Vac (5 min) and stored at −80 °C before further analysis.

Enzymatic Release of *N*-Glycans. PNGase F is used to release glycans from glycoproteins after derivatization of sialic acids on a solid phase.[42,51] Briefly, protein (500 μg) was heated at 90−100 °C for 10 min and mixed with 200 μL of AminoLink plus resin, which was pre-conditioned with 500 μL of 1× binding buffer (2×). 1× binding buffer contains 10 mM sodium citrate and 5 mM sodium carbonate. The protein was conjugated to the resin in 1× binding buffer [4 h at room temperature (RT)], followed by adding 50 mM $NaCNBH_3$. After washing the resin with 1× PBS (500 μL, 3×), the sample was further incubated in 1× PBS for 4 h in the presence of 50 mM $NaCNBH_3$. The unreacted aldehydes remaining on the resin were blocked with 1 M Tris·HCl (pH 7.4). The 2,6-linked sialic acids were then derivatized with 0.25 M EDC (200 μL) and 0.25 M HBot (200 μL) in ethanol at 37 °C/1 h. After removing reagents and washing the resin with DI water, the 2,3-linked sialic acids were further modified with 1 M *p*-toluidine (pT) (500 μL).[50] After multiple washing steps as previously described,[42] the resin was treated with glycosidases to analyze fucose linkages or glycan compositions by MS.

Determination of the Fucosylation Linkage. The fucosylation linkage of glycoproteins conjugated to the resin can be further determined by fucosidase and MS (Figure 2). The linkage is resolved by α1-2 fucosidase, α1-2,3,4 fucosidase, or α1-2,4,6 fucosidase. The conjugated glycoprotein was aliquoted into three equal amounts and treated with three fucosidases. An aliquot was incubated in 50 unit of α1-2,3,4 fucosidase in 20 mM Tris·HCl (pH 6.8), 37 °C/30 min. *N*-Glycans were released by 0.2 μL of PNGase F in 200 μL of 20 mM NH_4HCO_3, 37 °C/overnight (Figure 2 step ①). The second aliquot was treated with 10 units of α1-2 fucosidase in 50 mM sodium acetate and 5 mM $CaCl_2$ (pH 5.5), 37 °C/1 h and then by PNGase F to release *N*-glycans (Figure 2 step ②). The third aliquot was treated with 10 units of α1-2,4,6 fucosidase under the same condition, and its *N*-glycans were released by PNGase F (Figure 2 step ③). The linkage of α1,2, α1,3, and α1,6 is thus determined.

Comparison of Fucosylation of Saliva Glycoproteins. Proteins are extracted from saliva according to the saliva protein extraction protocol. The proteins (1 mg) were used to determine the fucosylation linkage using a solid-phase chemoenzymatic method (Figure 2). The aliquot proteins (500 μg) were also digested with trypsin for the quantitative analysis of GTFs. The structure of glycans in HC, OD, and LC was compared for features that are specific to cancer.

Mass Spectrometry Analysis of Glycans and Glycopeptides. Following PNGase F incubation, glycans were eluted by centrifugation and further washed with 100 μL of HPLC water (twice). The total volume is approximately 400 μL, of which 2−4 μL is used for glycan analysis by Bruker AutoFlex MALDI-TOF/TOF-MS. Each sample is tested in 3−4 technical duplicates, with an average of 10,000 shots per measurement. Global proteins are analyzed by shotgun proteomics. Briefly, protein (500 μg) was dissolved in 8 M urea and treated with 12 mM Tris (2-carboxyethyl) phosphine hydrochloride (37 °C/1 h) and 16 mM iodoacetamide (RT/1 h in the dark). 10 μg of trypsin (Promega, Madison, WI, USA) was added to the protein after dilution (<1.5 M urea). Protein digestion was conducted overnight at 37 °C, and the peptides were further purified by C18 SPE (solid-phase extraction). *N*-Glycosite analysis was performed by solid-phase extraction of glycopeptide enrichment (SPEG)[52] as follows: the purified peptides were oxidized by 10 mM sodium periodate to couple glycopeptides to hydrazide beads. Glycan-containing glycopeptides are released by PNGase F. The deglycopeptides were analyzed by Thermo Scientific Orbitrap Fusion LC−MS, using the same parameters described in our previous work.[47]

qPCR Quantification of Fucosyltransferases in Lung Tissues. The fucosyltransferases of interest were quantitatively analyzed by q-PCR using an ABI 7500 Real-Time PCR instrument. The TRIzol method was used to extract total RNA from LC tissues and matched adjacent non-tumor tissues. The

https://doi.org/10.1021/acsomega.2c01193
ACS Omega 2022, 7, 17894−17906

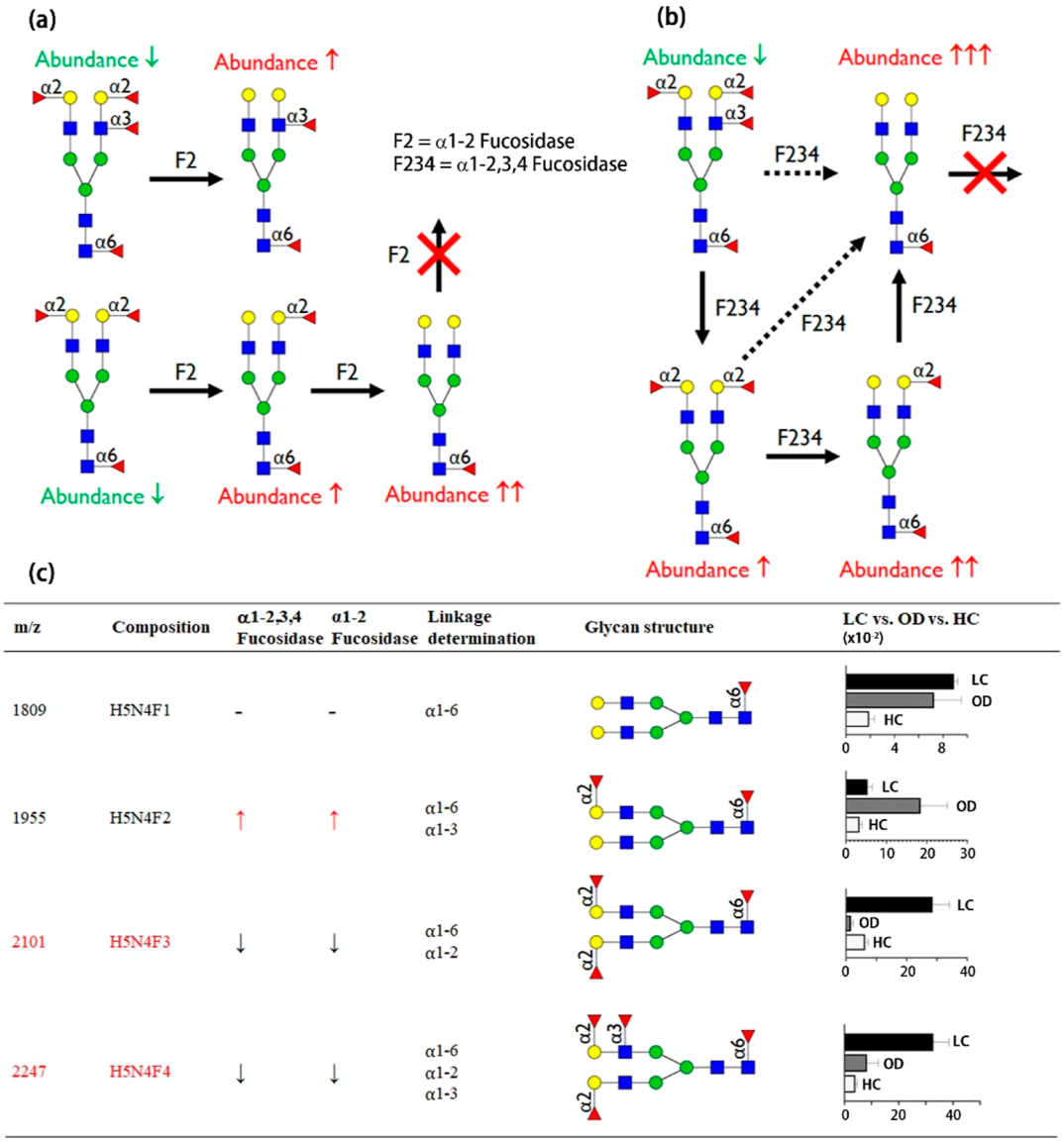

Figure 4. Description of the general workflow for the determination of linkage of fucosylated glycans containing multiple fucoses using different fucosidases. Saliva glycoproteins are extracted with lysis buffer and conjugated to the AminoLink Plus Resin. (a) Four fucosylated *N*-glycans (H5N4F4) contain α1-2 fucose on Gal after α1-2 fucosidase (F2) digestion, and the remaining fucose is either core α1-6 or antenna GlcNAc α1-3 linkage. F2 digestion can increase the abundance of H5N4F2, whereas H5N4F4 is reduced due to the loss of α1-2 fucose to form H5N4F2. Similarly, H5N4F3 loses two α1-2 fucose on Gal, and its abundance decreases accordingly. α1-2 fucosidase digestion eventually forms H5N4F1, whereas core α1-6 fucose still exists after F2 digestion. (b) α1-2,3,4 fucosidase (F234) determines the core-fucosylated glycan after removing α1-2, α1-3, and α1-4. H5N4F4 is trimmed to N5N4F3, N5H4F2, and H5N4F1. The abundance of these fucosylated glycans changes and is characterized by MALDI-MS. The remaining fucose of the glycan is a core fucose linkage. (c) Change in each glycan, H5N4F4, H5N4F3, H5N4F2, and H5N4F1, is the sum of these glycans and fucosidase digestion products in saliva. The reduction of H5N4F4 by F2 or F234 shows the presence of α1-2, α1-3, and α1-4. The ratio of LC vs OD. HC was a value measured from saliva glycoproteins without any fucosidase treatment. The arrow ↑ denotes the increase in abundance after fucosidase treatment compared with the untreated sample, and the arrow ↓ indicates decrease in abundance.

RNA concentration was measured using Nanodrop. The extracted RNA was reversed into cDNA using the RevertAid First Strand cDNA Synthesis kit (Thermo). The primer sequences for qPCR are shown in Supporting Information Table S2. We use human GAPDH as the reference gene. The reaction system is 10 μL 2× ChamQ Universal SYBR qPCR Master Mix, 0.4 μL of 10 μM upstream and downstream primers, 1 μL of cDNA template, and 20 μL of water for the final system. The reaction procedure of the qPCR system is as follows: pre-deformation at 95 °C for 30 s; 40 cycles of amplification (95 °C for 10 s and 60 °C for 30 s); and melting curve (60 °C for 60 s and 95 °C for 15 s). After the reaction, relative gene expression was calculated quantitatively by $2^{-\Delta\Delta Ct}$.

RESULTS

Protein Glycosylation Differs between Cancerous and Noncancerous Saliva. To show whether the glycosylation in the saliva of LC patients has changed, we performed SDS-PAGE on the saliva proteins of HC, other diseases (noncancer, OD), and LC (adenocarcinomas, LC) with and without glycosidase treatment. PNGase F (NEB BioLabs) is

https://doi.org/10.1021/acsomega.2c01193
ACS Omega 2022, 7, 17894−17906

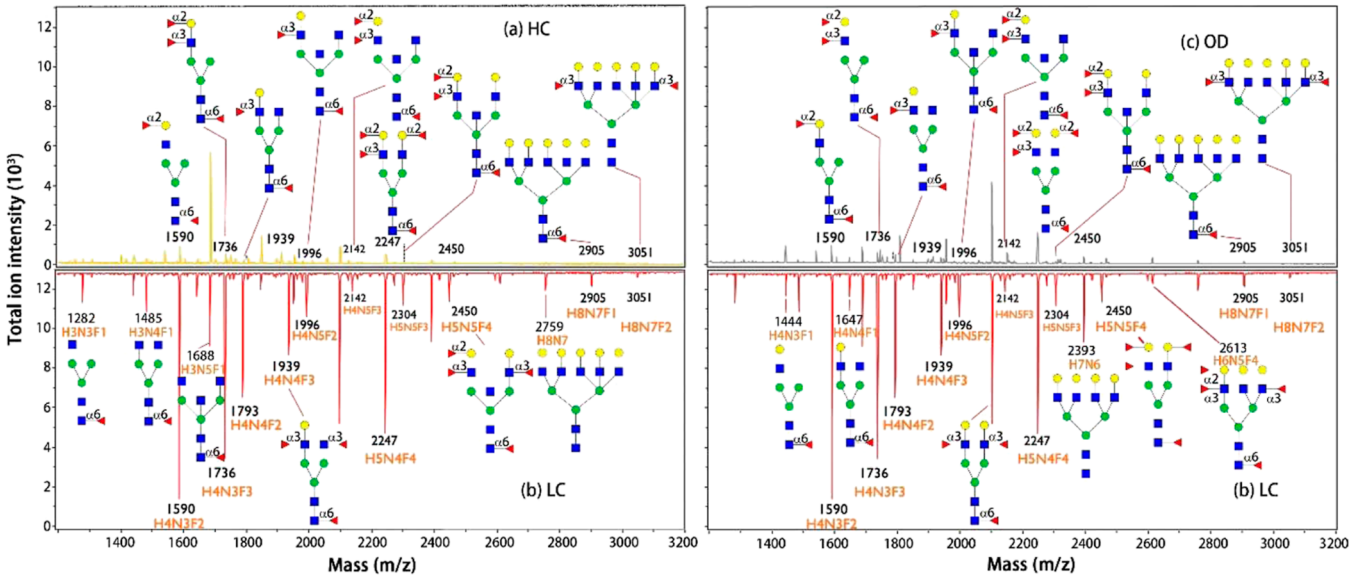

Figure 5. Different MALDI-MS glycan profiles of saliva glycoproteins in cancer compared with the HC and other disease. (a) Glycan from HC. The glycan abundance of protein in HC is significantly lower than that of LC. (b) Glycan profile of saliva glycoproteins of LC. The abundance of glycans with multiple fucosylation is significantly higher in cancer patients. These glycans also have core fucosylation, fucose on Gal or antenna GlcNAc. (c) Glycan profile of OD. The profile of OD is very different from that of LC. The characteristics of glycans can differentiate whether the patient is LC or OD.

an *N*-glycosidase that can cleave all *N*-glycans from glycoproteins but cannot cleave the innermost GlcNAc *N*-glycans with α1-3 fucose residue (e.g., plant or insect glycoproteins).[53] SDS-PAGE showed that HC has more protein bands between 66 and 95 kDa, OD has fewer intensity bands between 66 and 70 kDa, and LC has high intensity proteins between 52 and 66 kDa (Figure 3). The protein pattern between 52 and 30 kDa is also different. After PNGase F digestion, the protein bands of all samples shifted to lower molecular weight (MW), indicating the presence of *N*-glycosylation in HC, OD, and LC.

Fucosidase treatment can detect the presence of fucosylation on *N*-glycans or O-glycans, while fucosidase after PNGase F digestion can reveal whether there are fucoses on *N*-glycans. There was only a slight change when only fucosidase was used, but after treatment with both glycosidases, more pronounced protein bands appeared in OD and LC (Figure 3). These results indicate that fucosylation mainly occurs on *N*-glycosylation of LC, and *O*-glycosylation containing fucosylation is negligible. The specific linkage of fucosylation can be further determined by fucosidase.

Different Linkages of Fucosylated *N*-Glycans are Elevated in Lung Cancer. To determine the linkage of fucosylation, we used three fucosidases to process the glycoproteins on the solid support (resin) before PNGase F digestion. Because α1-2 fucosidase removes α1-2 fucose, the remaining linkage can be α1-3, α1-4, or α1-6. Similarly, α1-3 fucosidase can determine linkage α1-3, and the remaining linkage can be α1-2, α1-4, or α1-6. After α1-2,3,4 fucosidase digestion, any remaining fucose can be α1-6 core fucose. We used this strategy to elucidate the linkage of fucosylated *N*-glycans of saliva glycoproteins.

The glycan abundance after fucosidase treatment includes one that already exists in the sample and the other after corresponding fucose is removed. To explain our strategy, we used glycans with the same core structure H5N4 for quantitative analysis. As shown in Figure 4, the fucosylation linkage was determined by examining H5N4F4, H5N4F3, H5N4F2, and H5N4F1. The glycan profile of saliva glycoproteins indicates that these glycans are present in LC, so removing any fucose will alter the relative abundance of the related glycans. For example, α1-2 fucosidase (F2) digests H5N4F4 to H5N4F2 (corresponding to two α1-2 linkages), or H5N4F3 to H5N4F2 and H5N4F1 (Figure 4a). Similarly, α1-2,3,4 fucosidase (F234) alters H5N4F4 to H5N4F3, H5N4F2, and H5N4F1 (Figure 4b), resulting in the overall abundance of the final glycan profile (Figure 4c). The reduction of fucosylated glycans after F2 or F234 treatment indicates the presence of one or more of these fucosylation linkages in the sample. The core-fucosylated glycans were also identified because none of these fucosidases can digest α1-6 core fucosylation.

Elevated Fucosylation is Unique to Lung Cancer. To confirm whether the glycan profile can be used to distinguish between LC and OD/HC, we analyzed the overall profile of glycans of the saliva glycoproteins from patients (Supporting Information Table S1). The sample is processed on a solid support, and its sialic acids are stabilized by the ethyl esterification of α2,6-sialic acid and *p*-toluidine carbodiimide coupling of α2,3-sialic acid.[50] The *N*-glycans are characterized by MALDI-TOF/TOF-MS and analyzed by GlycoWorkBench.[54] Figure 5 shows the glycan profiles of saliva glycoproteins in HC, LC, and OD. Several conclusions can be drawn: (1) compared with LC, HC has a lower glycan abundance because the same amount of protein is conjugated to the resin. The highest peak observed in HC is H3N5F1 (1668 Da), and most glycans in LC are significantly higher than those in HC; (2) most glycans are core-fucosylated, that is, α1,6 fucosylation to the innermost GlcNAc. These glycans have significantly higher intensity, such as H3N3F1, H3N4F1, and H8N7F1; and (3) compared with HC or OD, the bisecting glycans with multiple fucosylation are obviously abundant in LC. These glycans include H4N3F3, H4N5F2, H4N5F3, H5N5F3, and H5N5F4; (4) there are multiple

https://doi.org/10.1021/acsomega.2c01193
ACS Omega 2022, 7, 17894−17906

Table 1. Regulation of Fucosylated Glycans of Saliva Glycoproteins in Lung Cancer Compared with Other Diseases and Healthy Controls[a]

Type	Core structure	Composition	Mass (m/z)	F234	F246	F2	Linkage	Glycan structure	Abundance (LC/OD/HC)
High mannose	Man3	H3N2	933.3	-	-	-	-		
		H3N2F1	1079.3	-	↑	-	α1-6		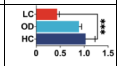
	Man4	H4N2	1095.3	-	↑	-	-		
		H4N2F1	1241.4	↑	↑	-	α1-6		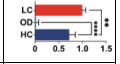
	Man5	H5N2	1257.4	-	↑	-	-		
		H5N2F1	1403.5	↑	↑	-	α1-6		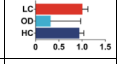
Hybrid	H5N3	H5N3	1460.5	-	↑	-	-		
		H5N3F1	1606.6	↑	↑	↑	α1-6		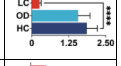
		H5N3F2	1752.6	↓	↓	↓	α1-6 α1-2		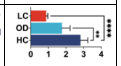
	H6N3	H6N3	1622.6	-	-	-	-		
		H6N3F1	1768.6	↑	↑	-	α1-6		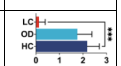
		H6N3F2	1914.7	↓	↓	-	α1-6 α1-3		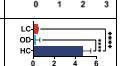
Complex	H4N3	H4N3	1298.4	-	↑	-	-		
		H4N3F1	1444.5	↑	↑	↑	α1-6		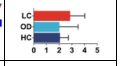
		H4N3F2	1590.6	↓	↓	↓	α1-6 α1-2		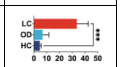
		H4N3F3	1736.6	↓	↓	↓	α1-6 α1-2 α1-3		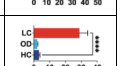
	H3N4	H3N4	1339.5	-	-	-	-		-
		H3N4F1	1485.5	-	↑	-	α1-6		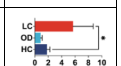
	H4N4	H4N4	1501.5	-	↑	-	-		-
		H4N4F1	1647.6	↑	↑	-	α1-6		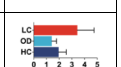
		H4N4F2	1793.6	↓	↓	-	α1-6 α1-3		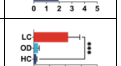
		H4N4F3	1939.7	↓	↓	↓	α1-6 α1-2 α1-3		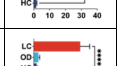
	H5N4	H5N4	1663.6	↑	↑	-	-		-
		H5N4F1	1809.6	-	↓	-	α1-6		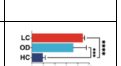
		H5N4F2	1955.7	↑	↓	↑	α1-6 α1-3		
		H5N4F3	2101.8	↓	↑	↓	α1-6 α1-2		
		H5N4F4	2247.8	↓	↓	↓	α1-6 α1-2 α1-3		

https://doi.org/10.1021/acsomega.2c01193
ACS Omega 2022, 7, 17894−17906

Table 1. continued

Type	Core structure	Composition	Mass (m/z)	F234	F246	F2	Linkage	Glycan structure	Abundance (LC/OD/HC)
	H3N5	H3N5	1542.6	↑	-	-	-		
		H3N5F1	1688.6	↑	↓	-	α1-6		
	H4N5	H4N5	1704.6	↑	-	-	-		
		H4N5F1	1850.7	↑	↓	-	α1-3		
		H4N5F2	1996.7	↓	↓	↑	α1-6 α1-3		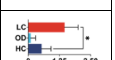
		H4N5F3	2142.8	↓	↓	↓	α1-6 α1-2 α1-3		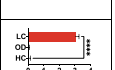
	H5N5	H5N5	1866.7	↑	-	-	-		-
		H5N5F1	2012.7	↑	↓	-	α1-3		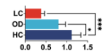
		H5N5F2	2158.8	↓	↓	↑	α1-6 α1-3		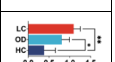
		H5N5F3	2304.8	↓	↑	↓	α1-6 α1-2 α1-3		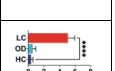
		H5N5F4	2450.9	↓	↓	-	α1-6 α1-2 α1-3		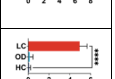
	H6N5	H6N5	2028.7	-	-	-	-		-
		H6N5F1	2174.8	↑	↓	↑	α1-6		
		H6N5F2	2320.8	↓	↓	↑	α1-6 α1-3		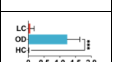
		H6N5F3	2466.9	↓	↑	↓	α1-6 α1-2 α1-3		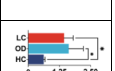
		H6N5F4	2612.9	↓	↓	↓	α1-6 α1-2 α1-3		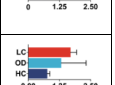
	H8N7	H8N7	2758.9	-	↑	-	-		
		H8N7F1	2905.1	↑	↓	-	α1-6		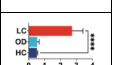
		H8N7F2	3051.1	↓	-	-	α1-3	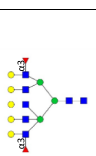	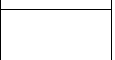

[a]The linkage of fucosylation is determined by fucosidases. The abundance between LC, OD, and HC is measured by MALDI-TOF/TOF-MS without any fucosidase treatment. The measurement is conducted in triplicate. H = Hex, N = HexNAc, F = Fucose, F234 = a1-2,3,4 Fucosidase, and F2 = a1-2 Fucosidase. The arrow ↑ and ↓ stand for increase or decrease in glycan after fucosidase treatment (10^{-2}). The intensity of each glycan is listed in Supporting Information Table S3 (* indicates statistical significance, *$P < 0.05$; **$P < 0.01$; ***$P < 0.001$; and ****$P < 0.0001$).

fucoses in core-GlcNAc (α1,6), antenna-GlcNAc (α1,3), and antenna-Gal (α1-2); and (5) the glycan profile of OD is also different from that of HC. For example, the highest peak in HC is H3N5F1, and in OD, it is H4N5F3. Generally, there are

https://doi.org/10.1021/acsomega.2c01193
ACS Omega 2022, 7, 17894−17906

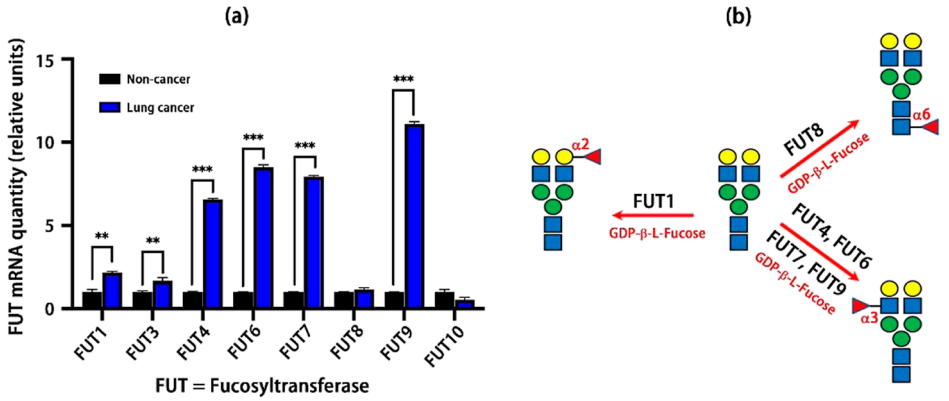

Figure 6. Biosynthetic pathway of formation of different fucosylation linkages by fucosyltransferase (FUT) enzymes through qPCR quantification. (a) qPCR quantification of FUT genes showed a substantial increase in FUT1 (2.17-fold), FUT3 (1.68), FUT4 (6.56), FUT6 (8.49), FUT7 (7.93), and FUT9 (11.09). The mRNA is extracted from lung tissues of adjacent non-tumors (control) and tumors; (b) FUT8 enzyme transfers GDP-β-L-fucose to the innermost GlcNAc, forming core-fucosylation (1.16-fold). The α1,2 linked fucosylation is catalyzed by FUT2, and the α1,3 linked fucosylation is catalyzed by the combination of FUT4, FUT6, and FUT9 enzymes.

several fucosylation of glycans in OD compared to HC. These results indicate that the characteristics of fucosylated glycans can be used as markers to detect whether a patient has LC or other diseases. The increase in fucosylated *N*-glycans is also shown in Supporting Information Figure S1. In general, the intensity of fucosylated *N*-glycans in LC is significantly higher than that in HC; interestingly, all of these glycans are core-fucosylated.

Changes in Different Types of *N*-Glycans. According to the branching of the *N*-glycan side chain, we divided fucosylated *N*-glycans into three different subtypes, namely, core-fucosylated high-mannose, fucosylated hybrid glycans, and fucosylated complex glycans. Supporting Information Figure S1 shows quantification of three subtypes of *N*-glycans. We found that changes in fucosylation occurred in high-mannose, hybrid, and complex glycans. Table 1 shows the quantitative analysis of major fucosylated *N*-glycans in saliva samples from HC, OD, and LC, including glycan type, core structure of its fucosylated glycan, mass (MW), fucosidase digestion (F234 and F2), glycan structure, and abundance of fucosylated glycan of saliva without fucosidase treatment. The core-fucosylation of Man3 (H3N2F1) decreased slightly in LC, but the changes in H4N2F1 and H5N2F1 were negligible. The core-fucosylated high-mannose (H3N2F1) was found in human saliva,[55] and their possible biosynthetic pathways may involve FUT8 and α-mannosidase I.[56] Compared with those in HC, the OD of fucosylated high-mannoses is significantly reduced. Therefore, understanding the biosynthetic pathway of core-fucosylated high-mannose may be helpful for the diagnosis of non-cancer diseases using saliva.

Hybrid glycans were detected in human saliva, and they were greatly reduced in LC (Table 1). The four fucosylated hybrid glycans H5N3F1, H5N3F2, H6N3F1, and H6N3F2 have much lower intensity in LC saliva. These glycans feature a core fucose, two of which have α1-2 fucose on Gal or α1-3 on GlcNAc. A similar trend was observed in gastric cancer serum, where the hybrid glycan H6N4F1 was downregulated in cancer serum.[57] How these hybrid glycans are regulated in tumorigenesis and cancer progression remain to be discovered, but they lack *N*-acetylglucosaminyltransferase I (GnT1), an enzyme responsible for the synthesis of hybrid and complex glycans, which can lead to delayed embryonic development.[58]

The most striking changes were observed in complex glycans with at least one fucose. We list 25 complex glycans that are significantly upregulated in LC (Table 1). Except for H3N5F1, H4N5F1, and H5N5F1, most of the glycans in LC are higher than those in OD or HC. The dominant increase in complex glycans is those with two or more fucoses, such as H4N3F2, H4N3F3, H4N4F2, H5N4F3, H5N4F4, H5N5F3, and H5N5F4. Because these complex glycans have core fucose, this suggests that the core fucosylation enzyme FUT8 is actively regulated in cancer. Studies have shown that the expression of FUT8 in tumor lesion is upregulated in NSCLC and is associated with tumor metastasis or malignancy.[59] According to the Human Protein Atlas, FUT8 protein is highly abundant in lung and digestive tract tissues, and its mRNA is highly expressed in salivary gland, tongue, and lung; however, proteomic analysis of saliva proteins did not detect FUT8 in HC, OD, or LC. These results suggest that the core-fucosylated proteins should come from the lungs or other organs. Additionally, the formation of α1,2-linked fucose on Gal or the formation of α1,3-linked fucose on GlcNAc was observed in saliva glycoproteins of LC patients. The increase in fucosylation specific for LC should be attributed to the increase in the expression of the corresponding fucosyltransferases (FUTs), which have been further characterized by qPCR.

Upregulated Fucosyltransferases Lead to Aberrant Fucosylation in Lung Cancer. To identify FUTs, we used clinical specimens form lung tumor tissue and matched adjacent non-tumor tissues to quantify the mRNA level of each FUT. To determine whether the saliva contains FUTs for synthesizing linkages of fucose, we used shotgun proteomics to analyze FUT expression in HC and LC. LC−MS/MS data showed that FUT6 and FUT11 were present in the saliva proteins of LC patients, but no other FUTs were identified from saliva; FUT4 and FUT6 were identified by SPEG and found in OD (Supporting Information Tables S4 and S5). In contrast, the abundance of mRNA extracted from saliva is extremely low. As a result, we did not observe any FUT mRNA expression using saliva samples.

Proteomic analysis of human saliva shows that there is an inherent correlation between the protein components of lung tissue and saliva. Literature studies have shown that when people suffer from LC, protein signature appears in human

https://doi.org/10.1021/acsomega.2c01193
ACS Omega 2022, 7, 17894−17906

saliva.[60] The presence of specific glycosylation can be traced back to lung tissue. To this end, we use qPCR to quantitatively characterize FUTs in lung tissues. As shown in Figure 6a, eight FUTs were found in adjacent non-tumor tissues (non-cancer) and tumor tissues (LC). Among these FUT genes, FUT4, FUT6, FUT7, and FUT9 are highly expressed in LC, while FUT1 and FUT3 have limited increase. Interestingly, the change in FUT8 mRNA levels between LC and HC is negligible, although the core-fucosylation in LC is significantly higher than that in HC.

The different linkages of fucosylation are regulated by specific FUT enzymes. Figure 6b schematically shows the biosynthetic pathway for fucosylation via various FUTs. Theoretically, FUT1 or FUT2 catalyzes GDP-β-L-fucose to Gal, forming α1,2-linked fucosylation.[61,62] mRNA expression indicates that FUT1 is an enzyme that synthesizes α1,2-linked fucosylation in lung tissues. FUT8 is responsible for the synthesis of α1,6-linked fucosylation and exists in LC and HC. FUT8 is associated with unfavorable clinical outcomes and may be a prognostic marker of LC.[63] FUT4, FUT6, and FUT9 are the three main isoforms that catalyze the α1,3-linked fucosylation in LC. Several *N*-glycans (Figure 5) have α1,2, α1,3, and α1,6-linked fucosylation, indicating that these FUTs are highly expressed in LC.

DISCUSSION

Our study shows that aberrant fucosylation is manifested in saliva glycoproteins of LC. The characteristics of fucosylated glycans are quite different from those of HCs or other diseases. Most glycans have increased core and antenna fucosylation in LC. Although many studies have reported the upregulation of α2,6-linked sialic acids in LC serum,[64,65] the increase in sialylation of LC saliva glycoproteins is negligible. The saliva glycoproteins, such as Mucin-5B, IgA, lactotransferrin, zinic-a2-glycoprotein, and so forth,[37] do possess sialic acid residues, but in our research, we found that dominant change is fucosylation. Our data show that the characteristics of fucosylation can distinguish whether a patient has LC or other diseases (Figure 5).

Because the tumor microenvironment alters the expression of glycoenzymes, abnormal fucosylation has been reported in various cancers. Importantly, fucosylation plays a vital role in cancer biology by regulating tumor signal transduction and cell−cell adhesion pathways and performs tumor immune surveillance through necrosis factor-related apoptosis-inducing ligand signaling.[66] Fucosylation analysis of prostate cancer cell lines showed that FUT1 is highly elevated compared to normal prostate cells and is regulated in LNCaP, so glycans carrying α1,3-linked fucose are elevated in prostate cancer.[67] Changes in the expression of fucosyltransferases (FUTs), FUT1, FUT3, FUT6, and FUT8, are associated with poor diagnosis and tumor metastasis in NSCLC.[68] Therefore, it is significant to identify FUTs in saliva and how this altered expression affects fucosylation.

The fucosylation is formed by transferring a GDP-β-L-fucose to the substrate catalyzed by a specific fucosyltransferase. As shown in Figure 6b, three different fucose linkages are catalyzed by the respective enzymes. It is known that FUT8 can synthesize α1,6 Fuc-GlcNAc, which is the core-fucosylated *N*-glycans. However, more than one FUT enzyme can catalyze the transfer of GDP-β-L-fucose to Gal or antenna GlcNAc. For instance, FUT1 is responsible for the synthesis of α1,2 Fuc-Gal, and any one of FUT4, FUT6, FUT7, and FUT9 can synthesize α1,3 Fuc-GlcNAc. Studies have shown that knocking down the FUT1 gene can attenuate tumor cell proliferation in HER2-overexpressed NCI-N87 cells.[69] Similarly, the upregulation of FUT1 in LC may lead to an increase in α1,2 fucosylation in LC saliva. In summary, our study shows that (1) FUT8 in LC leads to an increase in the level of core fucosylation, (2) FUT1 upregulation is the main driving factor for the significant increase in α1,2 linkage fucosylation, and (3) FUT4, FUT6, FUT7, and FUT9 are highly upregulated to elevate expression of α1,3 linked fucosylation.

Due to the unique characteristics of fucosylation in LC, the different glycan profiles between LC and HC/other disease can be used for the diagnosis of LC. Since each fucosylated glycoform can be recognized by a different lectin, a microarray or lectin-based enzyme-linked immunosorbent assay can be used to quantify and determine the fucosylated linkage. Our future work includes the use of lectins, such as lens culinaris agglutinin (LCA) (α1,6), ulex europaeus agglutinin I (UEAI) (α1,2), or aleuria aurantia lectin (AAL) (α1,2, α1,3, α1,4, and α1,6), to study linkage-specific glycoproteins. Additionally, collecting saliva from early patients may help determine the characteristics of fucosylation for early diagnosis.

CONCLUSIONS

Our study shows that aberrant fucosylation of saliva glycoproteins defines LC malignancy. Since the proteins in human biofluids are highly glycosylated, attempts are made to identify disease-specific markers through changes in protein glycosylation in biofluids. Abnormal glycosylation is usually produced by dysregulated glycoenzymes, which are responsible for adding or removing monosaccharides to or from glycans. The tumor microenvironment can cause glycoenzyme dysregulation that is very different from the normal pathophysiological state. Lung cancer tends to have higher FUT expression, leading to the upregulation of fucosylation. Glycoproteomics and glycomic analysis of saliva indicate that aberrant fucosylation is unique to LC, while other diseases (such as lung inflammatory) or HCs show a distinct fucosylation than LC. Our results confirmed that the increase in FUT1 expression enhanced α1,2-linked fucosylation, while FUT4,6,7,9 catalyzed the upregulation of α1,3-linked fucosylation. In contrast, FUT8 mRNA expression is also present in LC and adjacent non-tumor tissues, which indicates that FUT8 mRNA alone is not sufficient as a marker of LC, rather than using fucosylation patterns for tumor diagnosis.

ASSOCIATED CONTENT

Supporting Information

The Supporting Information is available free of charge at https://pubs.acs.org/doi/10.1021/acsomega.2c01193.

Reagents and materials; MALDI-TOF/TOF-MS analysis; LC−MS/MS analysis; saliva patient data; primer used for RT-PCR quantification; *N*-glycan abundances in HC, OD, and LC; saliva global proteins; saliva glycoproteins; salivary fucosylation in LC and HC; and fucosylation quantification (PDF)

AUTHOR INFORMATION

Corresponding Authors

Junhong Jiang − *Department of Pulmonary and Critical Care Medicine, The First Affiliated Hospital of Soochow University, Suzhou 215000, China; Department of Pulmonary and*

https://doi.org/10.1021/acsomega.2c01193
ACS Omega 2022, 7, 17894−17906

Critical Care Medicine, Dushu Lake Hospital, Affiliated to Soochow University, Suzhou 215000, China; Phone: (0512) 6262 7777; Email: jiangjunhong1969@suda.edu.cn

Shuang Yang − *Center for Clinical Mass Spectrometry, School of Pharmaceutical Sciences, Soochow University, Suzhou, Jiangsu 215123, China*; orcid.org/0000-0001-7958-0594; Phone: 13405064922; Email: yangs2020@suda.edu.cn

Authors

Ziyuan Gao − *Center for Clinical Mass Spectrometry, School of Pharmaceutical Sciences, Soochow University, Suzhou, Jiangsu 215123, China; Department of Pulmonary and Critical Care Medicine, The First Affiliated Hospital of Soochow University, Suzhou 215000, China*

Zhen Wu − *State Key Laboratory of Genetic Engineering, Department of Biochemistry, School of Life Sciences, Fudan University, Shanghai 200438, China*

Ying Han − *School of Life Science and Technology, ShanghaiTech University, Shanghai 201210, China*

Xumin Zhang − *State Key Laboratory of Genetic Engineering, Department of Biochemistry, School of Life Sciences, Fudan University, Shanghai 200438, China*

Piliang Hao − *School of Life Science and Technology, ShanghaiTech University, Shanghai 201210, China*; orcid.org/0000-0002-3632-1573

Mingming Xu − *Center for Clinical Mass Spectrometry, School of Pharmaceutical Sciences, Soochow University, Suzhou, Jiangsu 215123, China*; orcid.org/0000-0002-8158-2879

Shan Huang − *Center for Clinical Mass Spectrometry, School of Pharmaceutical Sciences, Soochow University, Suzhou, Jiangsu 215123, China*

Shuwei Li − *Nanjing Apollomics Biotech, Inc., Nanjing, Jiangsu 210033, China*

Jun Xia − *Department of Clinical Laboratory Center, Zhejiang Provincial People's Hospital, People's Hospital of Hangzhou Medical College, Hangzhou, Zhejiang 310014, China*

Complete contact information is available at: https://pubs.acs.org/10.1021/acsomega.2c01193

Author Contributions

Z.G.: formal analysis, investigation, visualization, and writing. Z.W.: MALDI-MS analysis and visualization. Y.H.: LC−MS/MS and visualization. X.Z.: resources, supervision, methodology, review, and editing. P.H.: resources, supervision, methodology, review, and editing. M.M.X.: investigation, visualization, supervision, and software. S.H.: investigation and visualization. S.W.L.: investigation, visualization, review, and editing. J.X.: resource, visualization, and review. J.H.J.: conceptualization, resources, funding acquisition, formal analysis, review, and editing. S.Y.: conceptualization, resources, funding acquisition, formal analysis, methodology, writing-original draft, writing-review, and editing.

Notes

The authors declare no competing financial interest.

■ ACKNOWLEDGMENTS

This work was supported by the startup funding of Soochow University, Jiangsu Province-Suzhou Science and Technology Planning Project SL T201917. We thank the Priority Academic Program Development of the Jiangsu Higher Education Institutes (PAPD).

■ REFERENCES

(1) Valverde, P.; Ardá, A.; Reichardt, N.-C.; Jiménez-Barbero, J.; Gimeno, A. Glycans in drug discovery. *MedChemComm* **2019**, *10*, 1678−1691.

(2) Rudd, P. M.; Elliott, T.; Cresswell, P.; Wilson, I. A.; Dwek, R. A. Glycosylation and the immune system. *Science* **2001**, *291*, 2370−2376.

(3) Saldova, R.; Fan, Y.; Fitzpatrick, J. M.; Watson, R. W. G.; Rudd, P. M. Core fucosylation and α2-3 sialylation in serum N-glycome is significantly increased in prostate cancer comparing to benign prostate hyperplasia. *Glycobiology* **2011**, *21*, 195−205.

(4) Höti, N.; Yang, S.; Hu, Y.; Shah, P.; Haffner, M. C.; Zhang, H. Overexpression of α (1,6) fucosyltransferase in the development of castration-resistant prostate cancer cells. *Prostate Cancer Prostatic Dis.* **2018**, *21*, 137−146.

(5) Roberts, P. C.; Garten, W.; Klenk, H. D. Role of conserved glycosylation sites in maturation and transport of influenza A virus hemagglutinin. *J. Virol.* **1993**, *67*, 3048−3060.

(6) Wan, H.; Gao, J.; Yang, H.; Yang, S.; Harvey, R.; Chen, Y.-Q.; Zheng, N.-Y.; Chang, J.; Carney, P. J.; Li, X.; Plant, E.; Jiang, L.; Couzens, L.; Wang, C.; Strohmeier, S.; Wu, W. W.; Shen, R.-F.; Krammer, F.; Cipollo, J. F.; Wilson, P. C.; Stevens, J.; Wan, X.-F.; Eichelberger, M. C.; Ye, Z. The neuraminidase of A (H3N2) influenza viruses circulating since 2016 is antigenically distinct from the A/Hong Kong/4801/2014 vaccine strain. *Nat. Microbiol.* **2019**, *4*, 2216−2225.

(7) Watanabe, Y.; Allen, J. D.; Wrapp, D.; McLellan, J. S.; Crispin, M. Site-specific glycan analysis of the SARS-CoV-2 spike. *Science* **2020**, *369*, 330−333.

(8) Wang, Y.; Wu, Z.; Hu, W.; Hao, P.; Yang, S. Impact of Expressing Cells on Glycosylation and Glycan of the SARS-CoV-2 Spike Glycoprotein. *ACS Omega* **2021**, *6*, 15988−15999.

(9) Gopaul, K. P.; Crook, M. A. Sialic acid: A novel marker of cardiovascular disease? *Clin. Biochem.* **2006**, *39*, 667−681.

(10) Hart, G. W.; Slawson, C.; Ramirez-Correa, G.; Lagerlof, O. Cross talk between O-GlcNAcylation and phosphorylation: roles in signaling, transcription, and chronic disease. *Annu. Rev. Biochem.* **2011**, *80*, 825−858.

(11) Elbatrawy, A. A.; Kim, E. J.; Nam, G. O-GlcNAcase: Emerging Mechanism, Substrate Recognition and Small-Molecule Inhibitors. *ChemMedChem* **2020**, *15*, 1244−1257.

(12) Hakomori, S.-i. Aberrant glycosylation in tumors and tumor-associated carbohydrate antigens. *Adv. Cancer Res.* **1989**, *52*, 257−331.

(13) Hakomori, S. Glycosylation defining cancer malignancy: New wine in an old bottle. *Proc. Natl. Acad. Sci. U.S.A.* **2002**, *99*, 10231−10233.

(14) Yin, H.; Lin, Z.; Nie, S.; Wu, J.; Tan, Z.; Zhu, J.; Dai, J.; Feng, Z.; Marrero, J.; Lubman, D. M. Mass-Selected Site-Specific Core-Fucosylation of Ceruloplasmin in Alcohol-Related Hepatocellular Carcinoma. *J. Proteome Res.* **2014**, *13*, 2887−2896.

(15) Yang, S.; Wang, P. G. Method development of glycoprotein biomarkers for cancers. *Bioanalysis* **2017**, *9*, 903−906.

(16) Shiiki, N.; Tokuyama, S.; Sato, C.; Kondo, Y.; Saruta, J.; Mori, Y.; Shiiki, K.; Miyoshi, Y.; Tsukinoki, K. Association between saliva PSA and serum PSA in conditions with prostate adenocarcinoma. *Biomarkers* **2011**, *16*, 498−503.

(17) Xu, M.; Hu, W.; Liu, Z.; Xia, J.; Chen, S.; Wang, P. G.; Yang, S. Glycoproteomic bioanalysis of exosomes by LC−MS for early diagnosis of pancreatic cancer. *Bioanalysis* **2021**, *13*, 861−864.

(18) Costa, A. F.; Campos, D.; Reis, C. A.; Gomes, C. Targeting Glycosylation: A New Road for Cancer Drug Discovery. *Trends Cancer* **2020**, *6*, 757.

(19) Chugh, S.; Gnanapragassam, V. S.; Jain, M.; Rachagani, S.; Ponnusamy, M. P.; Batra, S. K. Pathobiological implications of mucin

glycans in cancer: Sweet poison and novel targets. *Biochim. Biophys. Acta* **2015**, *1856*, 211−225.
(20) Chen, X.; Gole, J.; Gore, A.; He, Q.; Lu, M.; Min, J.; Yuan, Z.; Yang, X.; Jiang, Y.; Zhang, T.; Suo, C.; Li, X.; Cheng, L.; Zhang, Z.; Niu, H.; Li, Z.; Xie, Z.; Shi, H.; Zhang, X.; Fan, M.; Wang, X.; Yang, Y.; Dang, J.; McConnell, C.; Zhang, J.; Wang, J.; Yu, S.; Ye, W.; Gao, Y.; Zhang, K.; Liu, R.; Jin, L. Non-invasive early detection of cancer four years before conventional diagnosis using a blood test. *Nat. Commun.* **2020**, *11*, 3475.
(21) German, D. C.; Gurnani, P.; Nandi, A.; Garner, H. R.; Fisher, W.; Diaz-Arrastia, R.; O'Suilleabhain, P.; Rosenblatt, K. P. Serum biomarkers for Alzheimer's disease: proteomic discovery. *Biomed. Pharmacother.* **2007**, *61*, 383−389.
(22) Meany, D. L.; Sokoll, L. J.; Chan, D. W. Early detection of cancer: immunoassays for plasma tumor markers. *Expert Opin. Med. Diagn.* **2009**, *3*, 597−605.
(23) Patz, E. F.; Campa, M. J.; Gottlin, E. B.; Kusmartseva, I.; Guan, X. R.; Herndon, J. E. Panel of Serum Biomarkers for the Diagnosis of Lung Cancer. *J. Clin. Oncol.* **2007**, *25*, 5578.
(24) Kinney, J. S.; Morelli, T.; Braun, T.; Ramseier, C. A.; Herr, A. E.; Sugai, J. V.; Shelburne, C. E.; Rayburn, L. A.; Singh, A. K.; Giannobile, W. V. Saliva/pathogen biomarker signatures and periodontal disease progression. *J. Dent. Res.* **2011**, *90*, 752−758.
(25) Yuan, X.; Yang, C.; He, Q.; Chen, J.; Yu, D.; Li, J.; Zhai, S.; Qin, Z.; Du, K.; Chu, Z.; Qin, P. Current and perspective diagnostic techniques for COVID-19. *ACS Infect. Dis.* **2020**, *6*, 1998−2016.
(26) Fakheran, O.; Dehghannejad, M.; Khademi, A. Saliva as a diagnostic specimen for detection of SARS-CoV-2 in suspected patients: a scoping review. *Infect. Dis. Poverty* **2020**, *9*, 100.
(27) Xiao, H.; Zhang, Y.; Kim, Y.; Kim, S.; Kim, J. J.; Kim, K. M.; Yoshizawa, J.; Fan, L.-Y.; Cao, C.-X.; Wong, D. T. W. Differential Proteomic Analysis of Human Saliva using Tandem Mass Tags Quantification for Gastric Cancer Detection. *Sci. Rep.* **2016**, *6*, 22165.
(28) Verhoeven, Y.; Tilborghs, S.; Jacobs, J.; De Waele, J.; Quatannens, D.; Deben, C.; Prenen, H.; Pauwels, P.; Trinh, X. B.; Wouters, A.; Smits, E. L. J.; Lardon, F.; van Dam, P. A. The potential and controversy of targeting STAT family members in cancer. *Semin. Cancer Biol.* **2020**, *60*, 41−56.
(29) Tye, H.; Kennedy, C. L.; Najdovska, M.; McLeod, L.; McCormack, W.; Hughes, N.; Dev, A.; Sievert, W.; Ooi, C. H.; Ishikawa, T.-o.; Oshima, H.; Bhathal, P. S.; Parker, A. E.; Oshima, M.; Tan, P.; Jenkins, B. J. STAT3-driven upregulation of TLR2 promotes gastric tumorigenesis independent of tumor inflammation. *Cancer Cell* **2012**, *22*, 466−478.
(30) Zhang, S.; Yang, Y.; Huang, S.; Deng, C.; Zhou, S.; Yang, J.; Cao, Y.; Xu, L.; Yuan, Y.; Yang, J.; Chen, G.; Zhou, L.; Lv, Y.; Wang, L.; Zou, X. SIRT1 inhibits gastric cancer proliferation and metastasis via STAT3/MMP-13 signaling. *J. Cell. Physiol.* **2019**, *234*, 15395−15406.
(31) Rapado-González, Ó.; Martínez-Reglero, C.; Salgado-Barreira, N.; Takkouche, B.; Muinelo-Romay, L. Salivary biomarkers for cancer diagnosis: a meta-analysis. *Ann. Med.* **2020**, *52*, 131−144.
(32) Xiao, H.; Zhang, L.; Zhou, H.; Lee, J. M.; Garon, E. B.; Wong, D. T. W. Proteomic analysis of human saliva from lung cancer patients using two-dimensional difference gel electrophoresis and mass spectrometry. *Mol. Cell. Proteomics* **2012**, *11*, M111.012112.
(33) Wang, X.; Kaczor-Urbanowicz, K. E.; Wong, D. T. Salivary biomarkers in cancer detection. *Med. Oncol.* **2017**, *34*, 7.
(34) Sun, Y.; Huo, C.; Qiao, Z.; Shang, Z.; Uzzaman, A.; Liu, S.; Jiang, X.; Fan, L.-Y.; Ji, L.; Guan, X.; Cao, C.-X.; Xiao, H. Comparative Proteomic Analysis of Exosomes and Microvesicles in Human Saliva for Lung Cancer. *J. Proteome Res.* **2018**, *17*, 1101−1107.
(35) Smith, A. M. V.; Scott-Anne, K. M.; Whelehan, M. T.; Berkowitz, R. J.; Feng, C.; Bowen, W. H. Salivary glucosyltransferase B as a possible marker for caries activity. *Caries Res.* **2007**, *41*, 445−450.
(36) Gonzalez-Begne, M.; Lu, B.; Liao, L.; Xu, T.; Bedi, G.; Melvin, J. E.; Yates, J. R., III Characterization of the Human Submandibular/Sublingual Saliva Glycoproteome Using Lectin Affinity Chromatography Coupled to Multidimensional Protein Identification Technology. *J. Proteome Res.* **2011**, *10*, 5031−5046.
(37) Cross, B. W.; Ruhl, S. Glycan recognition at the saliva - oral microbiome interface. *Cell. Immunol.* **2018**, *333*, 19−33.
(38) Tenovuo, J. O.; Levine, M. J. *Human Saliva: Clinical Chemistry and Microbiology*; CRC Press: Boca Raton, FL, 1989.
(39) Madsen, J.; Mollenhauer, J.; Holmskov, U. Review: Gp-340/DMBT1 in mucosal innate immunity. *Innate Immun.* **2010**, *16*, 160−167.
(40) Güssow, D.; Rein, R.; Ginjaar, I.; Hochstenbach, F.; Seemann, G.; Kottman, A.; Ploegh, H. L. The human beta 2-microglobulin gene. Primary structure and definition of the transcriptional unit. *J. Immunol.* **1987**, *139*, 3132−3138.
(41) Jensen, P. H.; Karlsson, N. G.; Kolarich, D.; Packer, N. H. Structural analysis of N- and O-glycans released from glycoproteins. *Nat. Protoc.* **2012**, *7*, 1299−1310.
(42) Yang, S.; Hu, Y.; Sokoll, L.; Zhang, H. Simultaneous quantification of N- and O-glycans using a solid-phase method. *Nat. Protoc.* **2017**, *12*, 1229−1244.
(43) Riley, N. M.; Hebert, A. S.; Westphall, M. S.; Coon, J. J. Capturing site-specific heterogeneity with large-scale N-glycoproteome analysis. *Nat. Commun.* **2019**, *10*, 1311.
(44) Zacharias, L. G.; Hartmann, A. K.; Song, E.; Zhao, J.; Zhu, R.; Mirzaei, P.; Mechref, Y. HILIC and ERLIC Enrichment of Glycopeptides Derived from Breast and Brain Cancer Cells. *J. Proteome Res.* **2016**, *15*, 3624−3634.
(45) Xiao, H.; Chen, W.; Smeekens, J. M.; Wu, R. An enrichment method based on synergistic and reversible covalent interactions for large-scale analysis of glycoproteins. *Nat. Commun.* **2018**, *9*, 1692.
(46) Yang, S.; Wang, Y.; Mann, M.; Wang, Q.; Tian, E.; Zhang, L.; Cipollo, J. F.; Ten Hagen, K. G.; Tabak, L. A. Improved online LC-MS/MS identification of O-glycosites by EThcD fragmentation, chemoenzymatic reaction, and SPE enrichment. *Glycoconj. J.* **2021**, *38*, 145.
(47) Yang, S.; Onigman, P.; Wu, W. W.; Sjogren, J.; Nyhlen, H.; Shen, R.-F.; Cipollo, J. Deciphering Protein O-Glycosylation: Solid-Phase Chemoenzymatic Cleavage and Enrichment. *Anal. Chem.* **2018**, *90*, 8261−8269.
(48) Malaker, S. A.; Pedram, K.; Ferracane, M. J.; Bensing, B. A.; Krishnan, V.; Pett, C.; Yu, J.; Woods, E. C.; Kramer, J. R.; Westerlind, U.; Dorigo, O.; Bertozzi, C. R. The mucin-selective protease StcE enables molecular and functional analysis of human cancer-associated mucins. *Proc. Natl. Acad. Sci. U.S.A.* **2019**, *116*, 7278−7287.
(49) Reiding, K. R.; Blank, D.; Kuijper, D. M.; Deelder, A. M.; Wuhrer, M. High-throughput profiling of protein N-glycosylation by MALDI-TOF-MS employing linkage-specific sialic acid esterification. *Anal. Chem.* **2014**, *86*, 5784−5793.
(50) Yang, S.; Jankowska, E.; Kosikova, M.; Xie, H.; Cipollo, J. Solid-Phase Chemical Modification for Sialic Acid Linkage Analysis: Application to Glycoproteins of Host Cells Used in Influenza Virus Propagation. *Anal. Chem.* **2017**, *89*, 9508−9517.
(51) Yang, S.; Li, Y.; Shah, P.; Zhang, H. Glycomic Analysis Using Glycoprotein Immobilization for Glycan Extraction. *Anal. Chem.* **2013**, *85*, 5555−5561.
(52) Zhang, H.; Li, X.-j.; Martin, D. B.; Aebersold, R. Identification and quantification of N-linked glycoproteins using hydrazide chemistry, stable isotope labeling and mass spectrometry. *Nat. Biotechnol.* **2003**, *21*, 660−666.
(53) Tretter, V.; Altmann, F.; Kubelka, V.; März, L.; Becker, W. M. Fucose α1, 3-linked to the core region of glycoprotein N-glycans creates an important epitope for IgE from honeybee venom allergic individuals. *Int. Arch. Allergy Immunol.* **1993**, *102*, 259−266.
(54) Ceroni, A.; Maass, K.; Geyer, H.; Geyer, R.; Dell, A.; Haslam, S. M. GlycoWorkbench: a tool for the computer-assisted annotation of mass spectra of glycans. *J. Proteome Res.* **2008**, *7*, 1650−1659.
(55) Sinevici, N.; Mittermayr, S.; Davey, G. P.; Bones, J.; O'Sullivan, J. Salivary N-glycosylation as a biomarker of oral cancer: A pilot study. *Glycobiology* **2019**, *29*, 726−734.

https://doi.org/10.1021/acsomega.2c01193
ACS Omega 2022, 7, 17894−17906

(56) Nanno, Y.; Shajahan, A.; Sonon, R. N.; Azadi, P.; Hering, B. J.; Burlak, C. High-mannose type N-glycans with core fucosylation and complex-type N-glycans with terminal neuraminic acid residues are unique to porcine islets. *PLoS One* **2020**, *15*, No. e0241249.
(57) Ozcan, S.; Barkauskas, D. A.; Ruhaak, L.; Torres, J.; Cooke, C. L.; An, H. J.; Hua, S.; Williams, C. C.; Dimapasoc, L. M.; Han Kim, J.; Camorlinga-Ponce, M.; Rocke, D.; Lebrilla, C. B.; Solnick, J. V. Serum glycan signatures of gastric cancer. *Cancer Prev. Res.* **2014**, *7*, 226−235.
(58) Ioffe, E.; Stanley, P. Mice lacking N-acetylglucosaminyltransferase I activity die at mid-gestation, revealing an essential role for complex or hybrid N-linked carbohydrates. *Proc. Natl. Acad. Sci. U.S.A.* **1994**, *91*, 728−732.
(59) Chen, C.-Y.; Jan, Y.-H.; Juan, Y.-H.; Yang, C.-J.; Huang, M.-S.; Yu, C.-J.; Yang, P.-C.; Hsiao, M.; Hsu, T.-L.; Wong, C.-H. Fucosyltransferase 8 as a functional regulator of nonsmall cell lung cancer. *Proc. Natl. Acad. Sci. U.S.A.* **2013**, *110*, 630−635.
(60) Xiao, H.; Zhang, L.; Zhou, H.; Lee, J. M.; Garon, E. B.; Wong, D. T. Proteomic analysis of human saliva from lung cancer patients using two-dimensional difference gel electrophoresis and mass spectrometry. *Mol. Cell. Proteomics* **2012**, *11*, M111.012112.
(61) Goupille, C.; Marionneau, S.; Bureau, V.; Hallouin, F.; Meichenin, M.; Rocher, J.; Le Pendu, J. α1, 2Fucosyltransferase increases resistance to apoptosis of rat colon carcinoma cells. *Glycobiology* **2000**, *10*, 375−382.
(62) Tan, K.-P.; Ho, M.-Y.; Cho, H.-C.; Yu, J.; Hung, J.-T.; Yu, A. L.-T. Fucosylation of LAMP-1 and LAMP-2 by FUT1 correlates with lysosomal positioning and autophagic flux of breast cancer cells. *Cell Death Dis.* **2016**, *7*, No. e2347.
(63) Honma, R.; Kinoshita, I.; Miyoshi, E.; Tomaru, U.; Matsuno, Y.; Shimizu, Y.; Takeuchi, S.; Kobayashi, Y.; Kaga, K.; Taniguchi, N.; Dosaka-Akita, H. Expression of fucosyltransferase 8 is associated with an unfavorable clinical outcome in non-small cell lung cancers. *Oncology* **2015**, *88*, 298−308.
(64) Zhang, Z.; Wuhrer, M.; Holst, S. Serum sialylation changes in cancer. *Glycoconj. J.* **2018**, *35*, 139−160.
(65) Vasseur, J. A.; Goetz, J. A.; Alley, W. R., Jr.; Novotny, M. V. Smoking and lung cancer-induced changes in N-glycosylation of blood serum proteins. *Glycobiology* **2012**, *22*, 1684−1708.
(66) Zhang, B.; Roosmalen, I. A. M.; Reis, C. R.; Setroikromo, R.; Quax, W. J. Death receptor 5 is activated by fucosylation in colon cancer cells. *FEBS J.* **2019**, *286*, 555−571.
(67) Fukushima, K.; Satoh, T.; Baba, S.; Yamashita, K. α1,2-Fucosylated and β-N-acetylgalactosaminylated prostate-specific antigen as an efficient marker of prostatic cancer. *Glycobiology* **2009**, *20*, 452−460.
(68) Park, S.; Lim, J. M.; Chun, J. N.; Lee, S.; Kim, T. M.; Kim, D. W.; Kim, S. Y.; Bae, D. J.; Bae, S. M.; So, I. Altered expression of fucosylation pathway genes is associated with poor prognosis and tumor metastasis in non-small cell lung cancer. *Int. J. Oncol.* **2020**, *56*, 559−567.
(69) Kawai, S.; Kato, S.; Imai, H.; Okada, Y.; Ishioka, C. Suppression of FUT1 attenuates cell proliferation in the HER2-overexpressing cancer cell line NCI-N87. *Oncol. Rep.* **2013**, *29*, 13−20.

https://doi.org/10.1021/acsomega.2c01193
ACS Omega 2022, 7, 17894−17906